Flare Build-up and Preflare Activity at Microwave Region

K. Shibasaki (NRO)

Flare Scenario

1. energy storage in mag. field (current)
2. trigger (instabilities)
3. conversion of stored energy to other forms

(acceleration of particles, heating of plasma
generation of shock waves and mass motions)

Flare Build-up Study (FBS/SMY, SMA) 1975 – 1986

- coordinated observations and analysis
- wide energy band
  high spatial resolution
  high temporal resolution
- SMM (HXiS, XRP, UVSP, C/P), Hinotori
  VLA
  Vector Magnetographs
  ⋮

Build-up and Preflare Activities

- magnetic field — shear, emerging flux
- Hα — filament activation, eruption
- coronagraph (C/P) — CME starts before flare
- UV, soft X-ray — brightening
- hard X-ray — early onset (2 min.)
- microwave — intensity and polarization increase
  polarization reversal

Circumstantial evidences of magnetic reconnection

lack of important data

still not fully solved

(small flares)

Microwave Emission Mechanisms

Thermal f-f emission

$$\tau^{o} = 2 \times \frac{N_9^{2} \cdot L_9}{f_9^{2} \cdot T_6^{3/2}}$$

$\tau = 1$: $f_9 = 17$, $T_6 = 2$, $\underbrace{N_9 = 20}_{\text{high density}}$, $L_9 = 1$

Thermal gyro-resonance

$f = n \times f_H$ polarization $= T_b^{x} - T_b^{o}$

n: integer (2 or 3); f_H: gyrofrequency

$L = \left(\frac{v}{c}\right) L_H$

$\frac{v}{c}$: thermal velocity ~ 0.01; L_H: $|B / \mathrm{grad}\, B|$

$n = 3$ $f_9 = 17$ $\underbrace{B_3 = 2}_{\text{strong magnetic field}}$

$\tau = KL$ $K = K(\underline{\theta}, \underline{N_e}, \underset{x,\,o}{\underline{\underline{mode}}}, \lambda, T_e)$

Nonthermal gyro-synchrotron emission

high energy electrons

Maser

Microwave Observation

- high density plasma in the corona and the transition region
  - f-f emission
- strong magnetic field in the corona
  - gyro-resonance emission
- high energetic non-thermal electrons
  - gyro-synchrotron emission

Combination with other observations helps to identify these emission mechanisms

soft X-ray, hard X-ray, magnetic field, ...

Polarimeter

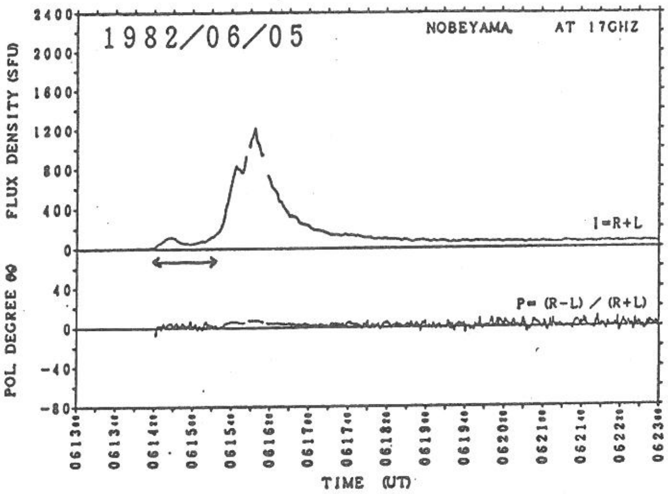

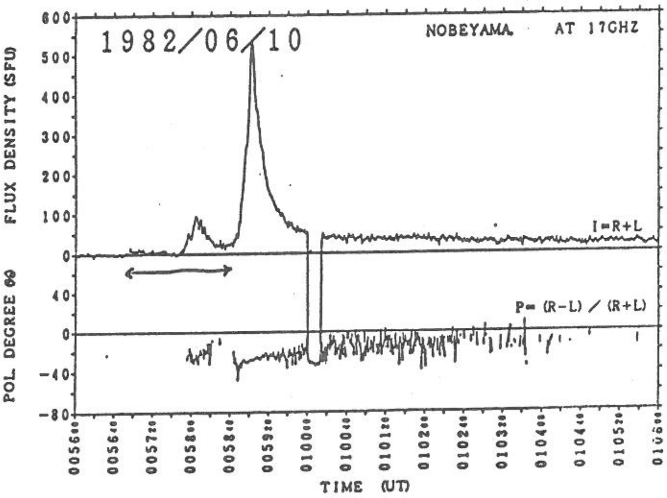

1-D interferometer   17 GHz

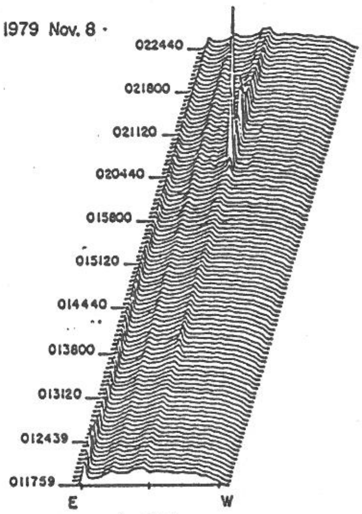

Fig. 1. A small burst preceding the large burst at 02h02m UT on November 8, 1979 at 1°3 east of the center. The bursts are presented on successively superposed east-west contours. Each of the contours is processed with a 40-s integration from the observed 40 Fourier components with a Hamming data window. Times are indicated on the left in UT (in order of hours, minutes, and seconds). Here, R and L are the right and left handed circular polarizations respectively.

Kai, Nakajima, Kosugi (1983)

· Statistical Study of Preflare Activity

(Kai, Najima and Kosugi, 1983)

97 events at 17 GHz

preflare ~25% (burst > 10 sfu)

~50% (burst > 500 sfu)

· preflare activities are low altitude phenomena

over the limb bursts start without preactivity

Two-dimensional High Spatial Resolution Observations of Flare Precurser

Review by Kundu Adv. Space Res. 6 (1986)

Event of June 25, 1980, 15:50 UT (1B/M4)

· change of the sense of polarization (μ-wave)
· filament eruption (Hα)
· flare near pol. reversal
· no photospheric mag. field change

Event of May 14, 1980, 19:20 UT

· bright emission E-W neutral line
↓
N-S neutral line
suggesting new system of loops by reconnection

Event of May 1, 1983, 22:55 UT

· additional component just before onset
suggesting appearance of emerging flux region

Event of October 1, 1980, 15:06 UT

Event of November 14, 1981, 19:20 UT

Activities in non-flaring active region

- variability
- non-thermal sources

what is different ?

flare related activity $\Longleftrightarrow$ non flare related activi

Cyclotron line emission

Polarization Reversal

No. 3, 1985

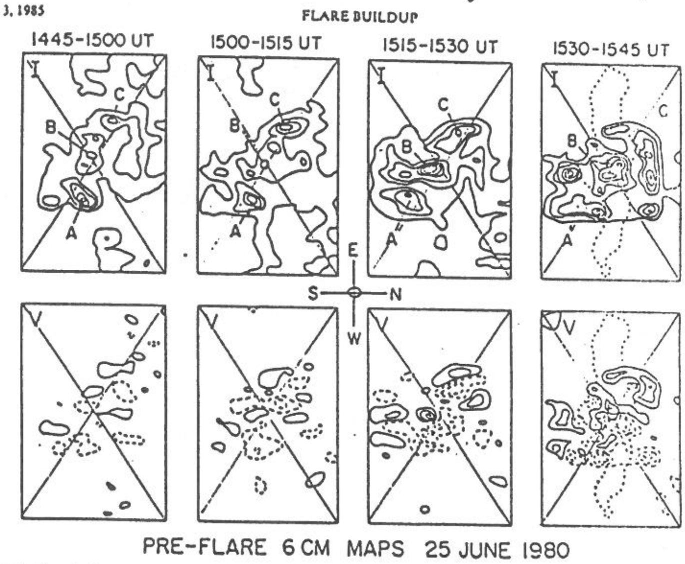

FIG. 1.—Central (1'.1 × 1'.6) regions of the 15 minute VLA synthesis maps at 6 cm wavelength between 14:45 and 15:45 UT. The maps are the Stokes intensity (I) and circular polarization (V). Note the polarization flux near the center of the last map. The dotted curve shows the maximum of the subsequent burst mapped at the VLA (Kundu et al. 1982).

compact. variable source

(5''
30-60 min
0.5-3×10⁵ K
<80 G

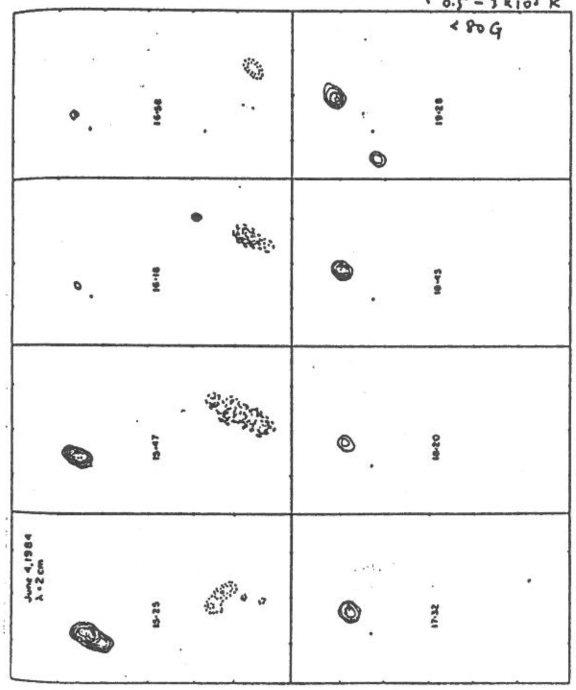

Willson and Lang

ApJ. 308 (1986)

588 SHEVGAONKAR AND KUNDU ApJ 342 (1989)

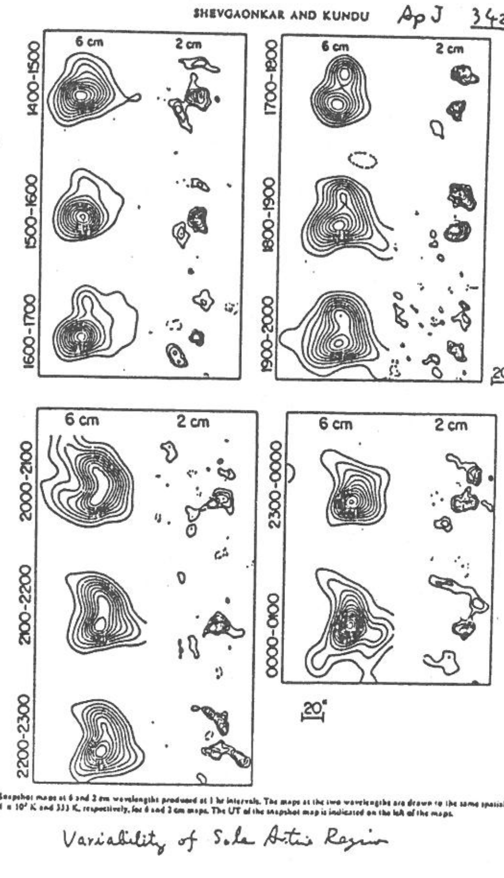

FIG. 3.—Snapshot maps at 6 and 2 cm wavelengths produced at 1 hr intervals. The maps at the two wavelengths are drawn to the same spatial scale. The contour interval is 3.4 × 10³ K and 333 K, respectively, for 6 and 2 cm maps. The UT of the snapshot map is indicated on the left of the maps.

Variability of Solar Active Region

MICROWAVE EMISSION ABOVE STEADY AND MOVING SUNSPOTS

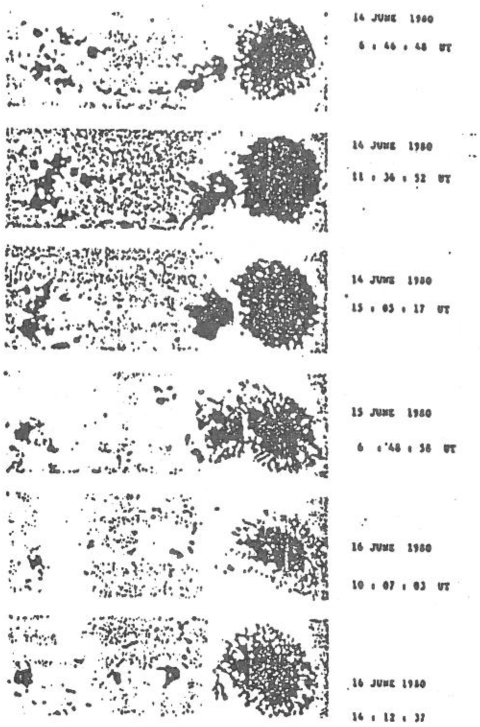

Fig. 5. Evolution of the sunspot group in AR 2502 as observed in white light at Debrecen Observatory, Hungary (Courtesy of L. Geszelyi).

Merging Sunspot

K. SHIBASAKI ET AL. Solar Phys. (1983

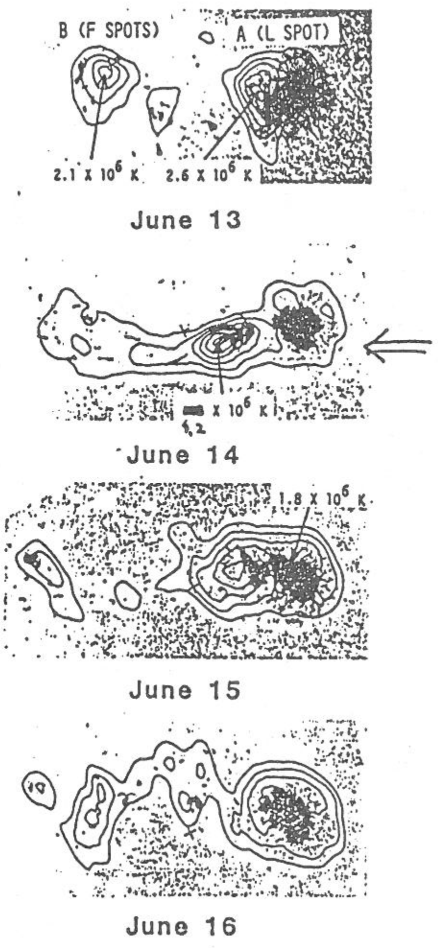

Fig. 2. Overlays of radio intensity maps on the sunspots in offband Hα. The contour interval is 5×10^5 K. The photographs are taken at Big Bear Solar Observatory (courtesy of Dr F. Tang).

Bright Component above merging sunspot

Observations by Nobeyama Radioheliograph

Characteristics of the instruments

- spatial resolution ~10"
- temporal resolution 50msec (25msec R, 25msec L)
- long observing time (6 hours/day)
- wide field of view (whole sun)
- mapping capability of large structure (short baseline)
- high dynamic range (large number of Fourier components)
  1567 complex components

We will study build-up and preflare activities,

- statistically,
- togather with high quality data sets,
  (Hα, mag. field, soft X-ray, hard X-ray.)
- in larger scale,
- of δ-type sunspots,
- of large and energetic flares,
- in transition region (only microwave)
- also non flare related activities
- :